Nano Research

ISSN 1998-0124 CN 11-5974/O4
https://doi.org/10.1007/s12274-021-3374-3

Research Article

Construction of poly-naphthalocyanine linked by [4]-radialene-like structures on silver surfaces

Rongting Wu[1,§,†], De-Liang Bao[1,§], Linghao Yan[1], Junhai Ren[1], Yanfang Zhang[1], Qi Zheng[1], Ye-Liang Wang[1], Qing Huan[1] (✉), Shixuan Du[1,2,3] (✉), and Hong-Jun Gao[1,2]

[1] *Institute of Physics & University of Chinese Academy of Sciences, Chinese Academy of Sciences, Beijing 100190, China*
[2] *CAS Center for Excellence in Topological Quantum Computation, Chinese Academy of Sciences, Beijing 100190, China*
[3] *Songshan Lake Materials Laboratory, Dongguan 523808, China*
[†] *Present address: Department of Applied Physics, Yale University, New Haven 06511, USA*
[§] *Rongting Wu and De-Liang Bao contributed equally to this work.*

Received: 1 December 2020 / **Revised:** 21 January 2021 / **Accepted:** 31 January 2021

ABSTRACT

Cyclic-conjugated linkages between planar-macrocyclic molecules contribute to the robustness of the two-dimensional (2D) polymerization and extension of π-interactions. The fabrication of such linkages in 2D polymers remains challenging. Combining scanning tunneling microscope (STM) measurements and density functional theory (DFT) calculations, we demonstrate a linear polymerization of metal-free naphthalocyanine (NPc) molecules with [4]-radialene-like linkages on silver surfaces. Experimentally, by depositing NPc molecules on the Ag(110) surface and subsequent annealing up to 750 K, one-dimensional polymers are constructed along the [1$\bar{1}$0] direction. High-resolution STM images show a stem-leaf-like feature. STM simulations based on a linear polymer of NPc molecules linked by four-membered carbon rings, [4]-radialene-like structure, agree well with the experimental observations. DFT calculations reveal that the polymerization process includes detaching two-terminal H atoms of NPc molecules along [1$\bar{1}$0] direction, then bonding with a neighboring dehydrogenated NPc molecule by forming a four-membered ring. The dehydrogenation process can be promoted by on-surface impurities such as additional H atoms. Similar polymerizations have been achieved on Ag(111) surfaces in an amorphous way. Moreover, the energy gap of the NPc molecule decreases after linear polymerization, suggesting a red-shift for its optical absorption/scattering spectrum. Our study offers a new route to polymerize conjugated molecules with extended planar π-interactions.

KEYWORDS

polymerization, naphthalocyanine, π-interaction extension, scanning tunneling microscope, density functional theory calculation

1 Introduction

Two-dimensional (2D) molecular polymerization, a method by which planar molecules are connected and form 2D networks, is widely used in the synthesis of novel 2D molecular crystals [1–4]. Using this method, researchers can create new 2D molecular crystals by extending zero-dimensional (0D) molecules to one-dimensional (1D) linear structures or 2D periodic structures on surfaces [5–9]. Furthermore, they can synthesize heterostructures comprising 2D molecular crystals and 2D materials [10, 11]. Such heterostructures are candidates for the construction of next-generation nanodevices [12]. It is worth mentioning that, in addition to the building blocks (the molecules), the linkages between molecules play dominant roles in controlling both the mechanical and electronic properties of the polymers [1]. The controlled polymerization of specific molecules utilizing unique linkages is always a desired technique for 2D-molecular-polymerization development [13].

So far, diverse linkages such as C–C single or double bonds [7, 14–16], C–metal coordinate bonds [17, 18], and/or B–O ring-like structures [19, 20] have been demonstrated. Because of the flexibility and rotatability of between-single-atoms bonds, on-surface polymers with such bonds usually show amorphous morphology and are difficult to transfer to other platforms for further investigations. In contrast, cyclic-conjugated linkages, e.g. radialene-like linkages (carbon polygons), show superior performance in both forming robust poly-structures and improving the optical or electronic properties of the individual molecules [21, 22]. The [4]-radialene-like linkages in pentacene oligomers have been predicted to not only serve as effective connectors between pairs of incoming spin edge channels, but also act as topological spin switches for the two outgoing channels [23]. In addition, the energy gaps of the conjugated systems can be reduced due to extended π-interactions, suggesting red-shifted light adsorption and enhanced light-harvesting efficiency [24].

As a group of versatile conjugated molecules, porphyrin and its derivatives, e.g. tetraphenylporphyrin (TPP) and 2,3-naphthalocyanine (NPc), have been widely studied [25–31] due to their advantageous electronic and optical properties. Though their polymerization by flexible C–C single bonds [32–35] and/or ring-like conjugated linkages [19, 36–38] using special precursors has been achieved, it is still a great challenge to directly polymerize them with cyclic-conjugated linkages. Here,

Address correspondence to Qing Huan, huanq@iphy.ac.cn; Shixuan Du, sxdu@iphy.ac.cn

we report the construction of linear NPc polymer linked by [4]-radialene-like structures using NPc molecule as the precursor. Direct deposition of NPc molecules on Ag(110) surface at room temperature results in the formation of a self-assembled monolayer. Post annealing up to 750 K leads to linear structures with a stem-leaf-like morphology observed in high-resolution scanning tunneling microscope (STM) images. Theoretical simulations demonstrate that the atomic configuration of the linear structure is head-to-head polymerized NPc molecules linked by four-membered carbon rings, i.e. [4]-radialene like structures. Further density functional theory (DFT) calculations reveal a stepwise mechanism that includes dehydrogenation and following polymerization. On-surface H atoms can significantly reduce the energy barrier for dehydrogenation. A similar polymerization process is also achieved on Ag(111). DFT calculations show that the polymer has a reduced energy gap compared with the monomer.

2 Methods

2.1 Experimental

All experiments were carried out in a homemade ultrahigh vacuum (UHV) variable temperature STM system [39] with the base pressure better than 2.0×10^{-10} mbar. The single crystals Ag(110) and Ag(111) (roughness < 0.03 μm, orientation accuracy < 0.1°, MaTeck Company) were prepared in vacuum by repeated cycles of Ne+ sputtering and subsequent annealing at 770 K until a clean and atomically flat surface was confirmed by STM imaging [40]. 2,3-Naphthalocyanine (Aldrich 95+%) in powder form was purified by a sublimation process with a homemade Knudsen cell (K-cell) evaporator in high vacuum for three days, followed by degassing at 640 K for 2 h under UHV condition [27]. The NPc was evaporated at 610 K, while the substrate Ag(110) and Ag(111) were kept at room temperature. Post annealing of these samples at 750 K could active the polymerization reaction of the NPc molecules on the silver surfaces.

2.2 Calculational

DFT calculations were performed using the Vienna *ab initio* simulation package (VASP) code [41, 42] with the projector-augmented wave (PAW) method [43]. The Perdew–Burke–Ernzernhof (PBE) [44] version of the generalized gradient approximation (GGA) [45] was used. HSE06 hybridized function [46] was used to calculate the energy gaps of NPc-molecule monomer, dimer, and polymer. The energy cutoff was 400 eV. Climbing-image-nudged-elastic-band (CI-NEB) calculations [47] were carried out to unveil the nature of the dehydrogenation process. For the benzene/Ag(110) model, the supercell contained five layers of Ag atoms to simulate the substrate and a benzene molecule on one side of the slab. The vacuum slab was about 16 Å thick. The lattice parameters of the supercell in calculations were 16.6 Å × 20.6 Å. For the NPc/Ag(110) system, to save calculation resources, the supercell contained two layers of Ag atoms and an NPc molecule on one side. The lattice parameters were 33.2 Å × 32.3 Å. The bottom two layers (benzene/Ag(110)) and one layer (NPc/Ag(110)) of Ag atoms were fixed, and all other atoms were fully relaxed until the intra-atomic forces were smaller than 0.02 eV/Å in the structural relaxations and 0.05 eV/Å in the CI-NEB calculations, respectively. The Brillouin zone was sampled with only the Γ-point in all calculations. Van der Waals interactions were included using Grimme's [48] empirical correction scheme. STM simulations were obtained from the optimized polymerized structures based on the Tersoff-Hamman approximation. Considering a blunt or molecule-decorated STM tip and the vibration of molecules/polymers at room temperature, a two-dimensional Gaussian filtering with a standard deviation $\sigma \approx 1.2$ Å was carried out to generate a comparable resolution between experimental and theoretical results.

3 Results and discussion

Experimentally, we found that the NPc molecules form a monolayer self-assembled structure after directly deposited onto the Ag(110) surface at room temperature (Fig. 1(a)). Similar to those on Ag(111) surface [49–51], NPc molecules exhibit cross-like shapes and pack together like mechanical gears. Two domains with the same unit cell but different molecular orientations are observed, as shown in Fig. 1(a) separated by the white dashed line. Interestingly, molecules present different self-assembly chiralities as highlighted by the green and blue gear-like symbols in domains 1 and 2, respectively. After annealing to 750 K, the morphology of the self-assembled NPc monolayer changes dramatically. Despite desorption, some remnant NPc molecules form ordered linear structures on the surface, as highlighted by the black dashed lines in Fig. 1(b). Notably, all linear structures are along the high-symmetry [1$\bar{1}$0] direction with identical space in between. Schematic models of self-assembled and polymerized NPc film are shown in Figs. 1(c) and 1(d), respectively.

The high-resolution STM image of the linear structure (Fig. 2(e)) exhibits a stem-leaf-like morphology, with the continuous dim "stem" along the [1$\bar{1}$0] direction (white dashed line) and discrete bright "leaves" in between (black dashed ellipses). According to the cross-cut profile along the linear structure (green line in Fig. 1(b)) shown in the upper panel of Fig. 2(a), the distance

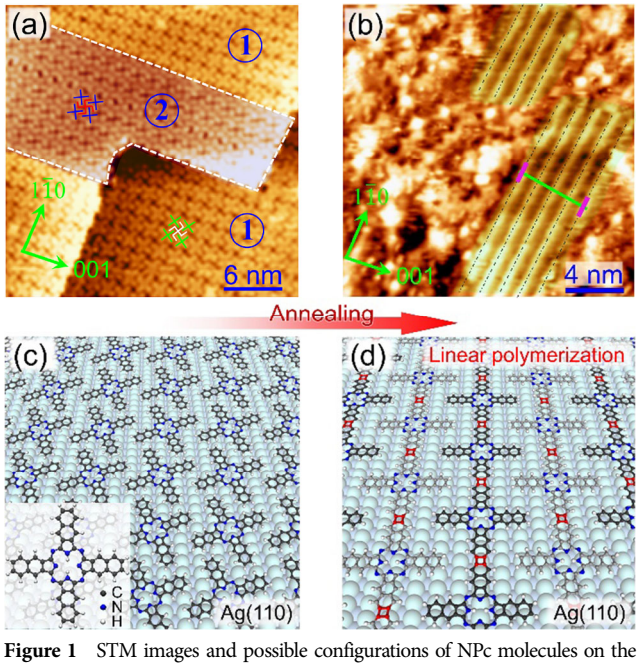

Figure 1 STM images and possible configurations of NPc molecules on the Ag(110) surface before and after annealing. (a) STM image of monolayer self-assembled NPc molecules on Ag(110) surface at room temperature. Closely packed NPc molecules represent a gear-like structure. (b) STM image of NPc molecules on Ag(110) surface after annealing at 750 K. Domains highlighted by black dashed lines show linear structures along the [1$\bar{1}$0] direction. (c) Schematic of the gear-like adsorption structure of NPc on Ag(110). Inset: optimized structure of single NPc molecule with a length of 1.98 nm. (d) Schematic of a proposed linearly polymeric structure of NPc after annealing. The neighboring NPc molecules are linked by [4]-radialene-like structure (red color), forming a molecular chain along the [1$\bar{1}$0] direction.

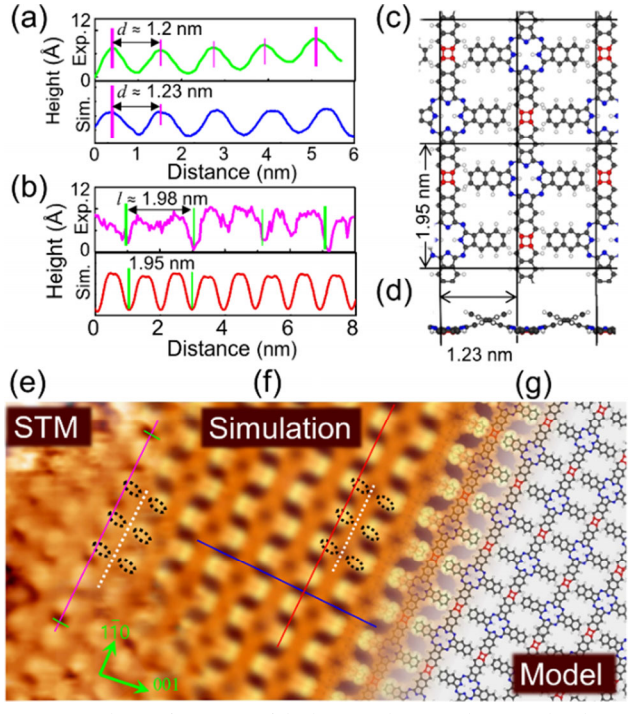

Figure 2 The configuration of the linear polymerized NPc molecules on the Ag(110) surface. (a) Upper: line profile of the green line shown in Fig. 1(b). Lower: line profile of the blue line in (f). (b) Upper: Line profile of the pink line in (e). Lower: line profile of the red line in (f). (c) The DFT relaxed structure of the linearly polymerized NPc molecules. The four-membered-carbon-ring linkages are highlighted in red. (d) Side view of the DFT relaxed structure. (e) High-resolution STM image of the linear structure shows a stem-leaf-like morphology (white dashed line and black dashed ellipses). (f) Simulated STM image. (g) The atomic model of the linear polymerized NPc molecules.

between the neighboring "stems" is about 1.2 nm, which equals 3 times the lattice constant of the Ag(110) surface along the [001] direction (0.41 nm). Furthermore, as shown in Fig. 2(b), the distance between every other "leaf" along the [1$\bar{1}$0] direction is about 1.98 nm, which matches the length of the NPc molecule, i.e. the distance between two outmost hydrogen atoms (1.98 nm). If the NPc molecules form a self-assembly structure, the distance between the two neighboring molecules along the linear structure should be about 2.48 nm considering the terminal H atoms and van der Waals interactions between neighbors, which is 0.5 nm longer than that obtained from the STM image, 1.98 nm. Therefore, the as-formed linear structure should be a head-to-head polymerized structure.

Based on the above analysis, we propose a structure of linearly polymerized NPc molecules, in which the neighboring molecules are linked by four-membered carbon rings (Figs. 2(c) and 2(d)). DFT calculations show that the relaxed inter-molecular distances are 1.95 and 1.23 nm along directions parallel and vertical to the polymerization direction, which agrees with the experimental measurements of 1.98 nm (Fig. 2(b)) and 1.2 nm (Fig. 2(a)), respectively. From the side view of the proposed model structure in Fig. 2(d), we find that the two unlinked lobes in each molecule upwarp from the surface after linear polymerization though the freestanding single molecule shows a planar structure. These upwarping flexible lobes might shake during scanning and deteriorate the resolution of STM image. STM simulations based on the relaxed structure are shown in Fig. 2(f). The linked lobes and the central part of the NPc molecule resemble the dim "stem" structure along the [1$\bar{1}$0] direction, marked as the white dashed line, while the unlinked lobes protrude from the dim "stem" and look like "leaves" as highlighted by black ellipses. Morphologically the simulation agrees with experimental STM very well. Two line profiles in the simulation image along two directions identical to those in experimental ones are drawn in lower panels in Figs. 2(a) and 2(b). The distance between the neighboring "stems" (blue) and that between every other "leaf" (red) are in line with those obtained from the experimental ones (upper panels of Fig. 2(a) and 2(b)). The agreement on both structural parameters and morphologies between simulations and experiments confirm that the structure observed in experiments is a linear NPc polymer with linkages of four-membered-carbon rings, i.e. [4]-radialene-like structure.

To reveal the formation mechanism of this linear polymer, CI-NEB calculations were performed based on the prototypes of benzene molecules on the Ag(110) surface, because the lobes of NPc molecules are basically benzene rings. As shown in Figs. 3(a)–3(d), the overall-polymerization process consists of four steps. In step I, one H atom is detached from the benzene skeleton to the substrate. If the H atom directly transfers from the C atom to the Ag substrate, the energy barrier is 2.39 eV, shown as the black lines in Fig. 3(a). In this case, the benzene molecule in the initial state lies flat on the surface (IS_1). It becomes tilted at transition state (TS_1) and finally bonds to the substrate through a C–Ag bond (FS_1). In step II, a second H atom, which is next to the first detached H, transfers from the benzene skeleton to the substrate with an energy barrier of 2.08 eV, shown as the black lines in Fig. 3(b). After this step,

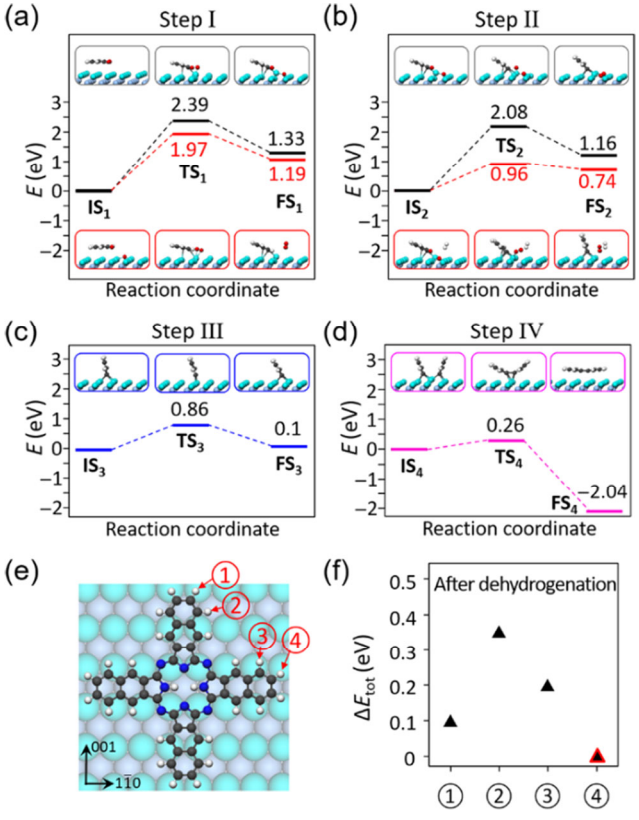

Figure 3 Mechanism of the formation of the four-membered-carbon ring on Ag(110) surface. (a)–(d) Energy profiles and related atomic models of the stepwise polymerization of benzene on Ag(110), including dehydrogenation of first H, dehydrogenation of second H, diffusion, and polymerization, respectively. Atomic models of the initial (IS), transition (TS), and final states (FS) are shown in the boxes with corresponding colors and labels. The red lines in (a) and (b) are pathways when an extra H adsorbed near benzene. (e) Top view of the NPc molecule adsorbed on Ag(110) surface. (f) Energy differences of the system after releasing corresponding H atoms marked in (e). The energy of configuration after detaching H④ is set to 0 eV as a reference.

the benzene forms two C–Ag bonds with the substrate and shows an increased tilted angle compared with that of FS_1.

It is worth mentioning that when an extra H atom adsorbs near the benzene molecule, the detached H atom can bind to the extra H atom and form an H_2 molecule. As a consequence, the dehydrogenation barriers with the extra H are reduced to 1.97 and 0.96 eV for steps I and II, respectively, shown as red lines in Figs. 3(a) and 3(b). The significantly decreased barriers suggest that the dehydrogenation process is sensitive to the surrounding conditions. Impurities represented by H adatoms facilitate the dehydrogenation process.

For step III, the dehydrogenated benzene molecule diffuses along the [1$\bar{1}$0] direction on Ag(110) surface with a barrier of 0.86 eV as shown in Fig. 3(c). When two dehydrogenated benzene molecules meet each other, the dehydrogenated parts lift, bind to each other, and form a four-membered-carbon-ring bond, i.e. a [4]-radialene-like structure, as shown in Fig. 3(d). The barrier of step IV is as low as 0.26 eV, followed by a 2.04 eV energy reduction.

Figure 3(e) shows the most stable adsorption configuration of an NPc molecule on the Ag(110) surface. There are four different detachable H atoms, as marked by ①, ②, ③, and ④. Figure 3(f) shows the energy differences of the systems after releasing different H atoms. It is clear that the release of H④ leads to the most stable structure. This result suggests that the [4]-radialene-like linkages prefer to be formed between NPc molecules along the [1$\bar{1}$0] channel, which is in accordance with the experimental observation.

Previous works about self-assembled NPc molecules on metal surfaces indicate a weak but non-negligible molecule–substrate interaction [49, 52]. The symmetry of the surface greatly affects the adsorption configuration of single molecules and self-assembled structures [53, 54]. To investigate the effect of substrate symmetry on the polymerization of NPc molecules, we carried out polymerization experiments on the Ag(111) surface.

Figure 4(a) shows the typical high-resolution STM image of self-assembled NPc monolayer on Ag(111) surface. The NPc molecules display cross-like shapes and pack together like mechanical gears on the surface. Six domains with different orientations and lattice parameters were observed on the surface [49]. Here the green arrows indicate the directions of single molecules, and the green dashed rectangle shows the unit cell. After annealed up to 750 K, the morphology of NPc monolayer film on Ag(111) surface also endured dramatic changes, as shown in Fig. 4(b). Albeit annealed at very high temperature, only a few (~ 30%) NPc molecules desorbed, and most of them remain on the surface forming disordered structures. Interestingly, all NPc molecules link together through lobes with neighboring molecules forming disordered 2D polymers. Besides the bended [32] or dislocated [55] polymerization as indicated by the green dashed lines, we also observed a linearly bonded dimer, as shown in the yellow square and zoom-in image in the inset. The inset STM image shows that the two molecules form a linear connection with an inter-space of 19.6 Å. This value is smaller than the calculated vdW length (19.8 Å) of one NPc molecule, suggesting the formation of chemical bonds between these two molecules.

Figure 4(e) shows the highly resolved STM image of the dimer. Noteworthy, the electronic density of states smoothly and seamlessly extends across the intermolecular junction with a protrusion at the center of the dimer. Figure 4(c) shows the optimized molecular model of the dimer with a [4]-radialene-like structure marked in red. Figure 4(d) is the simulated STM image at the same bias as the experimental STM image, showing similar protrusion at the center. Here, the optimized

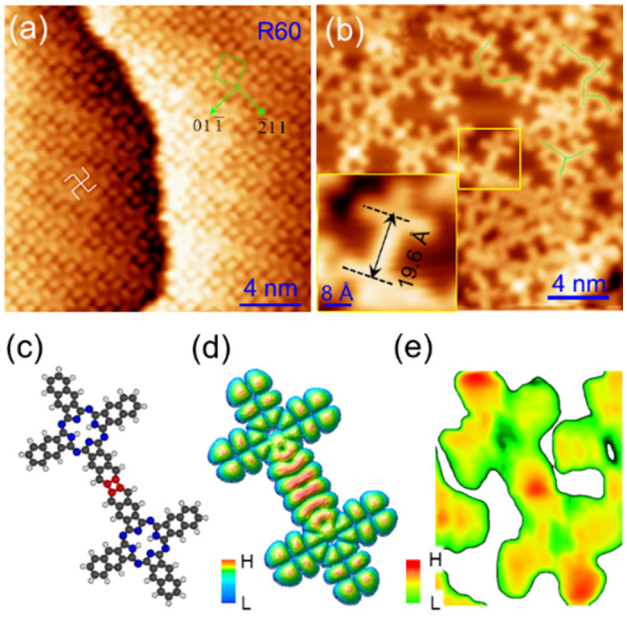

Figure 4 Polymerization of NPc molecules on the Ag(111) surface. (a) STM image of monolayer NPc molecules on Ag(111) surface. The NPc molecules are closely packed with a molecular gear-like structure. The green dashed rectangle represents the unit cell. (b) STM image of NPc molecules on Ag(111) surface after annealed at 750 K. All molecules are linked together with neighboring molecules by the lobes. The inset is the zoom-in STM image of the yellow square, showing a linearly linked NPc dimer, with the distance between the center of the two monomers of 19.6 Å. (c) Relaxed model of the dimer. (d) The simulated STM image of (c) shows a protrusion at the junction. (e) High-resolution STM image of the dimer, with a protrusion at the junction. The scanning parameters are −2.0 V and 0.1 nA in (a) and (b), −1.4 V and 0.1 nA in (e).

distance between two molecules is 19.5 Å, which coincides with the experimental data.

Further theoretical calculations reveal that the four-member-ring linked polymerization significantly reduces the energy gap (Fig. 5), thus offers a way to tune the light harvest efficiency. DFT calculations with HSE06 hybrid function show that the highest occupied molecular orbital (HOMO)–lowest unoccupied molecular orbital (LUMO) gaps are 1.37, 1.27, and 1.18 eV for monomer, dimer, and 2D patterns of linear polymers, respectively. The 2D linear NPc polymer has a gap reduction of ~ 0.2 eV referring to the NPc monomer. Typically, the absolute energy gaps for organic molecules calculated based on the HSE06 hybrid function are underestimated [56], while the relative differences are trustworthy. From the experimental absorption spectra of NPc molecules [57], where the absorption

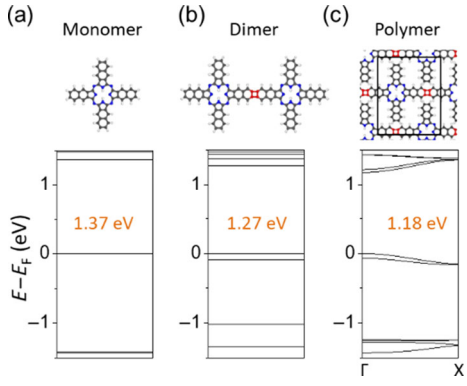

Figure 5 Configurations and band structures of monomer, dimer, and polymer of NPc molecules. (a)–(c) Top views of the atomic models (upper panels) and energy diagrams/band structures (lower panels) of monomer (a), dimer (b), and polymer (c) of NPc molecules, respectively.

peak is around 760 nm, we can infer that the energy gap of NPc is about 1.63 eV. Therefore, the energy gap for linear NPc polymer shifts to around 1.43 eV, which makes the polymer a superior candidate for photovoltaic applications [58]. The reduction of the energy gap via polymerization enables the tunability of NPc's optical absorption, resulting in a red-shifted absorption peak toward the near-infrared region.

4 Conclusion

In summary, by depositing NPc molecules on Ag(110) at room temperature and post-annealing to about 750 K, linear-polymerized NPc molecules have been constructed along the [1$\bar{1}$0] direction on Ag(110) surface. High-resolution STM images of the polymerized NPc molecules show a stem-leaf-like feature, which is confirmed by DFT calculations. The polymerization mechanism is rationalized as follows: The NPc molecules firstly dehydrogenate two-terminal H atoms in the [1$\bar{1}$0] direction of Ag(110), then diffuse along the channel until they meet another dehydrogenated NPc molecule. The four exposed C atoms bond together and form a four-membered C ring, i.e. a [4]-radialene-like linkage. The on-surface H atoms can significantly lower the energy barrier of the dehydrogenation. Conjugated-polymerization of NPc molecules is also achieved on Ag(111) substrate. The conjugated-polymerization of NPc molecules with [4]-radialene-like linkages effectively reduce the energy gap of NPc molecules. Our work offers a new cyclic-conjugate-linkage route for constructing linear-polymerized NPc molecules, which can be expanded to other macrocyclic-conjugated molecules and hold promising applications in photovoltaic systems.

Acknowledgments

We thank Prof. Werner Hofer and Prof. Sokrates T. Pantelides for helpful discussions and suggestions. This work was financially supported by the National Key Research and Development Program of China (No. 2016YFA0202300), the National Natural Science Foundation of China (Nos. 61888102 and 61725107), Strategic Priority Research Program of the Chinese Academy of Sciences (No. XDB30000000), the International Partnership Program of Chinese Academy of Sciences (No. 112111KYSB20160061), and China Postdoctoral Science Foundation (No. 2018M641511). DFT computations were carried out at the National Supercomputing Center of Tianjin.

References

[1] Colson, J. W.; Dichtel, W. R. Rationally synthesized two-dimensional polymers. *Nat. Chem.* **2013**, *5*, 453–465.

[2] Payamyar, P.; King, B. T.; Öttinger, H. C.; Schlüter, A. D. Two-dimensional polymers: Concepts and perspectives. *Chem. Commun.* **2016**, *52*, 18–34.

[3] Grill, L.; Hecht, S. Covalent on-surface polymerization. *Nat. Chem.* **2020**, *12*, 115–130.

[4] Schlüter, A. D. Mastering polymer chemistry in two dimensions. *Commun. Chem.* **2020**, *3*, 12.

[5] Cai, J. M.; Ruffieux, P.; Jaafar, R.; Bieri, M.; Braun, T.; Blankenburg, S.; Muoth, M.; Seitsonen, A. P.; Saleh, M.; Feng, X. L. et al. Atomically precise bottom-up fabrication of graphene nanoribbons. *Nature* **2010**, *466*, 470–473.

[6] Ruffieux, P.; Wang, S. Y.; Yang, B.; Sánchez-Sánchez, C.; Liu, J.; Dienel, T.; Talirz, L.; Shinde, P.; Pignedoli, C. A.; Passerone, D. et al. On-surface synthesis of graphene nanoribbons with zigzag edge topology. *Nature* **2016**, *531*, 489–492.

[7] Grill, L.; Dyer, M.; Lafferentz, L.; Persson, M.; Peters, M. V.; Hecht, S. Nano-architectures by covalent assembly of molecular building blocks. *Nat. Nanotechnol.* **2007**, *2*, 687–691.

[8] Sánchez-Sánchez, C.; Dienel, T.; Deniz, O.; Ruffieux, P.; Berger, R.; Feng, X. L.; Müllen, K.; Fasel, R. Purely armchair or partially chiral: Noncontact atomic force microscopy characterization of dibromo-bianthryl-based graphene nanoribbons grown on Cu(111). *ACS Nano* **2016**, *10*, 8006–8011.

[9] Zhong, D. Y.; Franke, J. H.; Podiyanachari, S. K.; Blömker, T.; Zhang, H. M.; Kehr, G.; Erker, G.; Fuchs, H.; Chi, L. F. Linear alkane polymerization on a gold surface. *Science* **2011**, *334*, 213–216.

[10] Gobbi, M.; Orgiu, E.; Samorì, P. When 2D materials meet molecules: Opportunities and challenges of hybrid organic/inorganic Van der Waals heterostructures. *Adv. Mater.* **2018**, *30*, 1706103.

[11] Jariwala, D.; Marks, T. J.; Hersam, M. C. Mixed-dimensional Van der Waals heterostructures. *Nat. Mater.* **2017**, *16*, 170–181.

[12] He, D. W.; Zhang, Y. H.; Wu, Q. S.; Xu, R.; Nan, H. Y.; Liu, J. F.; Yao, J. J.; Wang, Z. L.; Yuan, S. J.; Li, Y. et al. Two-dimensional quasi-freestanding molecular crystals for high-performance organic field-effect transistors. *Nat. Commun.* **2014**, *5*, 5162.

[13] Yun, H. J.; Choi, H. H.; Kwon, S. K.; Kim, Y. H.; Cho, K. Polarity engineering of conjugated polymers by variation of chemical linkages connecting conjugated backbones. *ACS Appl. Mater. Interfaces* **2015**, *7*, 5898–5906.

[14] Liu, W.; Luo, X.; Bao, Y.; Liu, Y. P.; Ning, G. H.; Abdelwahab, I.; Li, L. J.; Nai, C. T.; Hu, Z. G.; Zhao, D. et al. A two-dimensional conjugated aromatic polymer via C–C coupling reaction. *Nat. Chem.* **2017**, *9*, 563–570.

[15] Vasseur, G.; Abadia, M.; Miccio, L. A.; Brede, J.; Garcia-Lekue, A.; de Oteyza, D. G.; Rogero, C.; Lobo-Checa, J.; Ortega, J. E. Π band dispersion along conjugated organic nanowires synthesized on a metal oxide semiconductor. *J. Am. Chem. Soc.* **2016**, *138*, 5685–5692.

[16] Bi, S.; Yang, C.; Zhang, W. B.; Xu, J. S.; Liu, L. M.; Wu, D. Q.; Wang, X. C.; Han, Y.; Liang, Q. F.; Zhang, F. Two-dimensional semiconducting covalent organic frameworks via condensation at arylmethyl carbon atoms. *Nat. Commun.* **2019**, *10*, 2467.

[17] Wang, W. H.; Shi, X. Q.; Wang, S. Y.; Van Hove, M. A.; Lin, N. Single-molecule resolution of an organometallic intermediate in a surface-supported ullmann coupling reaction. *J. Am. Chem. Soc.* **2011**, *133*, 13264–13267.

[18] Ren, J. H.; Bao, D. L.; Dong, L.; Gao, L.; Wu, R. T.; Yan, L. H.; Wang, A. W.; Yan, J. H.; Wang, Y. L.; Huan, Q. et al. Lattice-directed construction of metal–organic molecular wires of pentacene on the Au(110) surface. *J. Phys. Chem. C* **2017**, *121*, 21650–21657.

[19] Spitler, E. L.; Dichtel, W. R. Lewis acid-catalysed formation of two-dimensional phthalocyanine covalent organic frameworks. *Nat. Chem.* **2010**, *2*, 672 – 677.

[20] Wan, S.; Guo, J.; Kim, J.; Ihee, H.; Jiang, D. L. A photoconductive covalent organic framework: Self-condensed arene cubes composed of eclipsed 2D polypyrene sheets for photocurrent generation. *Angew. Chem., Int. Ed.* **2009**, *48*, 5439–5442.

[21] Yang, S. J.; Chu, M.; Miao, Q. Connecting two phenazines with a four-membered ring: The synthesis, properties and applications of cyclobuta[1,2-*b*:3,4-*b*′]diphenazines. *J. Mater. Chem. C* **2018**, *6*, 3651–3657.

[22] Sanchez-Sanchez, C.; Nicolaï, A.; Rossel, F.; Cai, J. M.; Liu, J. Z.; Feng, X. L.; Müllen, K.; Ruffieux, P.; Fasel, R.; Meunier, V. On-surface cyclization of *ortho*-dihalotetracenes to four- and six-membered rings. *J. Am. Chem. Soc.* **2017**, *139*, 17617–17623.

[23] Cui, P.; Zhang, Q.; Zhu, H. B.; Li, X. X.; Wang, W. Y.; Li, Q. X.; Zeng, C. G.; Zhang, Z. Y. Carbon tetragons as definitive spin switches in narrow zigzag graphene nanoribbons. *Phys. Rev. Lett.* **2016**, *116*, 026802.

[24] Zhong, Y.; Cheng, B. R.; Park, C.; Ray, A.; Brown, S.; Mujid, F.; Lee, J. U.; Zhou, H.; Suh, J.; Lee, K. H. et al. Wafer-scale synthesis of monolayer two-dimensional porphyrin polymers for hybrid superlattices. *Science* **2019**, *366*, 1379–1384.

[25] Liljeroth, P.; Repp, J.; Meyer, G. Current-induced hydrogen tautomerization and conductance switching of naphthalocyanine molecules. *Science* **2007**, *317*, 1203–1206.

[26] Huan, Q.; Jiang, Y.; Zhang, Y. Y.; Ham, U.; Ho, W. Spatial imaging of individual vibronic states in the interior of single molecules. *J. Chem. Phys.* **2011**, *135*, 014705.

[27] Yan, L. H.; Wu, R. T.; Bao, D. L.; Ren, J. H.; Zhang, Y. F.; Zhang, H.

G.; Huang, L.; Wang, Y. L.; Du, S. X.; Huan, Q. et al. Adsorption behavior of Fe atoms on a naphthalocyanine monolayer on Ag(111) surface. *Chin. Phys. B* **2015**, *24*, 076802.
[28] Kobayashi, N.; Nakajima, S. I.; Ogata, H.; Fukuda, T. Synthesis, spectroscopy, and electrochemistry of tetra-*tert*-butylated tetraazaporphyrins, phthalocyanines, naphthalocyanines, and anthracocyanines, together with molecular orbital calculations. *Chem.—Eur. J.* **2004**, *10*, 6294–6312.
[29] Lim, B.; Margulis, G. Y.; Yum, J. H.; Unger, E. L.; Hardin, B. E.; Grätzel, M.; McGehee, M. D.; Sellinger, A. Silicon-naphthalo/phthalocyanine-hybrid sensitizer for efficient red response in dye-sensitized solar cells. *Org. Lett.* **2013**, *15*, 784–787.
[30] Pandey, R.; Kerner, R. A.; Menke, S. M.; Holst, J.; Josyula, K. V. B.; Holmes, R. J. Tin naphthalocyanine complexes for infrared absorption in organic photovoltaic cells. *Org. Electron.* **2013**, *14*, 804–808.
[31] Bao, D. L.; Zhang, Y. Y.; Du, S. X.; Pantelides, S. T.; Gao, H. J. Barrierless on-surface metal incorporation in phthalocyanine-based molecules. *J. Phys. Chem. C* **2018**, *122*, 6678–6683.
[32] Sun, Q.; Zhang, C.; Cai, L. L.; Xie, L.; Tan, Q. G.; Xu, W. On-surface formation of two-dimensional polymer via direct C-H activation of metal phthalocyanine. *Chem. Commun.* **2015**, *51*, 2836–2839.
[33] Lafferentz, L.; Eberhardt, V.; Dri, C.; Africh, C.; Comelli, G.; Esch, F.; Hecht, S.; Grill, L. Controlling on-surface polymerization by hierarchical and substrate-directed growth. *Nat. Chem.* **2012**, *4*, 215–220.
[34] Lin, T.; Shang, X. S.; Adisoejoso, J.; Liu, P. N.; Lin, N. Steering on-surface polymerization with metal-directed template. *J. Am. Chem. Soc.* **2013**, *135*, 3576–3582.
[35] Kuang, G. W.; Chen, S. Z.; Wang, W. H.; Lin, T.; Chen, K. Q.; Shang, X. S.; Liu, P. N.; Lin, N. Resonant charge transport in conjugated molecular wires beyond 10 nm range. *J. Am. Chem. Soc.* **2016**, *138*, 11140–11143.
[36] Abel, M.; Clair, S.; Ourdjini, O.; Mossoyan, M.; Porte, L. Single layer of polymeric Fe-phthalocyanine: An organometallic sheet on metal and thin insulating film. *J. Am. Chem. Soc.* **2011**, *133*, 1203–1205.
[37] Zhou, J.; Sun, Q. Magnetism of phthalocyanine-based organometallic single porous sheet. *J. Am. Chem. Soc.* **2011**, *133*, 15113–15119.
[38] Wang, Y.; Yuan, H.; Li, Y. F.; Chen, Z. F. Two-dimensional iron-phthalocyanine (Fe-Pc) monolayer as a promising single-atom-catalyst for oxygen reduction reaction: A computational study. *Nanoscale* **2015**, *7*, 11633–11641.
[39] Stipe, B. C.; Rezaei, M. A.; Ho, W. A variable-temperature scanning tunneling microscope capable of single-molecule vibrational spectroscopy. *Rev. Sci. Instrum.* **1999**, *70*, 137–143.
[40] Wu, R. T.; Ren, J. H.; Dong, L.; Wang, Y. L.; Huan, Q.; Gao, H. J. Quasi-free-standing graphene nano-islands on ag(110), grown from solid carbon source. *Appl. Phys. Lett.* **2017**, *110*, 213107.
[41] Vanderbilt, D. Soft self-consistent pseudopotentials in a generalized eigenvalue formalism. *Phys. Rev. B* **1990**, *41*, 7892–7895.
[42] Kresse, G.; Furthmüller, J. Efficient iterative schemes for *ab initio* total-energy calculations using a plane-wave basis set. *Phys. Rev. B* **1996**, *54*, 11169–11186.
[43] Kresse, G.; Joubert, D. From ultrasoft pseudopotentials to the projector augmented-wave method. *Phys. Rev. B* **1999**, *59*, 1758–1775.
[44] Perdew, J. P.; Burke, K.; Ernzerhof, M. Generalized gradient approximation made simple. *Phys. Rev. Lett.* **1996**, *77*, 3865–3868.
[45] Perdew, J. P.; Chevary, J. A.; Vosko, S. H.; Jackson, K. A.; Pederson, M. R.; Singh, D. J.; Fiolhais, C. Atoms, molecules, solids, and surfaces: Applications of the generalized gradient approximation for exchange and correlation. *Phys. Rev. B* **1992**, *46*, 6671–6687.
[46] Krukau, A. V.; Vydrov, O. A.; Izmaylov, A. F.; Scuseria, G. E. Influence of the exchange screening parameter on the performance of screened hybrid functionals. *J. Chem. Phys.* **2006**, *125*, 224106.
[47] Henkelman, G.; Uberuaga, B. P.; Jónsson, H. A climbing image nudged elastic band method for finding saddle points and minimum energy paths. *J. Chem. Phys.* **2000**, *113*, 9901–9904.
[48] Wu, X.; Vargas, M. C.; Nayak, S.; Lotrich, V.; Scoles, G. Towards extending the applicability of density functional theory to weakly bound systems. *J. Chem. Phys.* **2001**, *115*, 8748–8757.
[49] Wu, R. T.; Yan, L. H.; Zhang, Y. F.; Ren, J. H.; Bao, D. L.; Zhang, H. G.; Wang, Y. L.; Du, S. X.; Huan, Q.; Gao, H. J. Self-assembled patterns and young's modulus of single-layer naphthalocyanine molecules on Ag(111). *J. Phys. Chem. C* **2015**, *119*, 8208–8212.
[50] Wu, R. T.; Yan, L. H.; Bao, D. L.; Ren, J. H.; Du, S. X.; Wang, Y. L.; Huan, Q.; Gao, H. J. Self-assembly evolution of metal-free naphthalocyanine molecules on Ag(111) at the submonolayer coverage. *J. Phys. Chem. C* **2019**, *123*, 7202–7208.
[51] Wu, R. T.; Bao, D. L.; Yan, L. H.; Wang, Y. L.; Ren, J. H.; Zhang, Y. F.; Huan, Q.; Zhang, Y. Y.; Du, S. X.; Pantelides, S. T.; Gao, H. J. Direct visualization of hydrogen-transfer intermediate states by scanning tunneling microscopy. *J. Phys. Chem. Lett.* **2020**, *11*, 1536–1541.
[52] Pham, T. A.; Song, F.; Stöhr, M. Supramolecular self-assembly of metal-free naphthalocyanine on Au(111). *Phys. Chem. Chem. Phys.* **2014**, *16*, 8881–8885.
[53] Du, S. X.; Gao, H. J.; Seidel, C.; Tsetseris, L.; Ji, W.; Kopf, H.; Chi, L. F.; Fuchs, H.; Pennycook, S. J.; Pantelides, S. T. Selective nontemplated adsorption of organic molecules on nanofacets and the role of bonding patterns. *Phys. Rev. Lett.* **2006**, *97*, 156105.
[54] Sun, X. P.; Hyeon Ko, S.; Zhang, C.; Ribbe, A. E.; Mao, C. D. Surface-mediated DNA self-assembly. *J. Am. Chem. Soc.* **2009**, *131*, 13248–13249.
[55] Sun, Q.; Zhang, C.; Kong, H. H.; Tan, Q. G.; Xu, W. On-surface aryl-aryl coupling via selective C-H activation. *Chem. Commun.* **2014**, *50*, 11825–11828.
[56] Refaely-Abramson, S.; Sharifzadeh, S.; Jain, M.; Baer, R.; Neaton, J. B.; Kronik, L. Gap renormalization of molecular crystals from density-functional theory. *Phys. Rev. B* **2013**, *88*, 081204.
[57] El-Khouly, M. E.; El-Mohsnawy, E.; Fukuzumi, S. Solar energy conversion: From natural to artificial photosynthesis. *J. Photochem. Photobiol. C* **2017**, *31*, 36–83.
[58] Polman, A.; Knight, M.; Garnett, E. C.; Ehrler, B.; Sinke, W. C. Photovoltaic materials: Present efficiencies and future challenges. *Science* **2016**, *352*, aad4424.